Warm calibration unit of the mid-infrared ELT instrument METIS - overview of current status towards FDR

Monika Rutowska, Tarun Kumar Sharma, Michael Wiest,

Sabine Graf, Lucas Labadie, et al.

Published version information:

Citation: M Rutowska et al. Warm calibration unit of the mid-infrared ELT instrument METIS: overview and current status towards FDR. Proc SPIE 12184 (2022): 121843M. Is in proceedings of: Conference on Ground-Based and Airborne Instrumentation for Astronomy IX, Montréal, Québec, Canada, 17-22 Jul 2022

DOI: 10.1117/12.2630802

Warm calibration unit of the mid-infrared ELT instrument METIS: overview and current status towards FDR

Monika Rutowska, Tarun Kumar Sharma, Michael Wiest, Sabine Graf, Lucas Labadie, et al.

Monika Rutowska, Tarun Kumar Sharma, Michael Wiest, Sabine Graf, Lucas Labadie, Christian Straubmeier, Andreas Eckart, Stephen Todd, Tibor Agócs, Gert Raskin, Jan Goris, Marchel Gerbers, Leonard Burtscher, Roy van Boekel, Adrian Glauser, Jeffrey Lynn, Bernhard Brandl, Felix Bettonvil, "Warm calibration unit of the mid-infrared ELT instrument METIS: overview and current status towards FDR," Proc. SPIE 12184, Ground-based and Airborne Instrumentation for Astronomy IX, 121843M (29 August 2022); doi: 10.1117/12.2630802

SPIE.

Event: SPIE Astronomical Telescopes + Instrumentation, 2022, Montréal, Québec, Canada

Warm calibration unit of the mid-infrared ELT instrument METIS – overview of current status towards FDR

Monika Rutowska[a], Tarun Sharma[a], Michael Wiest[a], Sabine Graf[a], Lucas Labadie[a], Andreas Eckart[a], Christian Straubmeier[a], Stephen Todd[b], Tibor Agócs[c], Dirk Lesman[c], Remko Stuik[d], Gert Raskin[e], Jan Goris[e], Marchel Gerbers[c], Leonard Burtscher[d], Roy van Boekel[f], Adrian Glauser[g], Bernhard Brandl[c,d], and Felix Bettonvil[c,d]

[a]I. Physikalisches Institut, Universität zu Köln, Zülpicher Straße 77, 50937, Köln, Germany
[b]UK Astronomy Technology Centre, STFC, Royal Observatory, Edinburgh, EH9 3HJ, UK
[c]NOVA Optical Infrared Instrumentation Group at ASTRON, P.O. Box 2, 7990 AA Dwingeloo, The Netherlands
[d]Leiden Observatory, Leiden University, P.O. Box 9513, 2300 RA Leiden, The Netherlands
[e]KU Leuven, Instituut voor Sterrenkunde, Celestijnenlaan 200D, 3001 Leuven, Leuven, Belgium
[f]Max-Planck-Institut für Astronomie, Königstuhl 17, 69117, Heidelberg
[g]ETH Zürich, Institute for Particle Physics and Astrophysics, Wolfgang-Pauli-Strasse 27, CH-8093 Zürich, Switzerland

ABSTRACT

The warm calibration unit (WCU) is one of the subsystems of the future METIS instrument on the Extremely Large Telescope (ELT). Operating at room temperature, the WCU is mounted above the main cryostat of METIS. It will be employed as a calibration reference for science observations, as well as for verification and alignment purposes during the AIT phase. The WCU is designed and constructed at the University of Cologne, one of the partner in the METIS consortium. WCU recently went through a successful Optics Long Lead Items Review by ESO. Now, the WCU is entering the last phase of the project, the Final Design Review (FDR). In this paper, we present the current status of the WCU design and summarize the mechanical and system engineering work. We describe the design of the hexapod formed by six manually adjustable links and its interfaces with the METIS cryostat together with the CFRP-based optical bench and Invar-based optical mounts. Lab prototyping results of one actuator under a nominal load of 5 kN confirms the achievable high linear resolution (20 μm). We present the status of the WCU laser cabinet. We discuss the lastest progress in the laboratory testing of some WCU functionalities, such as the fibre-fed monochromatic sources for the spectral calibration of the LM-Spectrograph of METIS, and the spatial calibration sources using the integrating sphere. We detail the activities foreseen until FDR together with the preparation of the sub-system MAIT work.

Keywords: ELT, METIS, Warm Calibration Unit, mid-infrared, hexapod, alignment, calibration, AIT

1. INTRODUCTION

The METIS instrument is a part of the first-light instrument suite that will equip the new ELT towards the end of 2020s. The other first-light instruments are MICADO and HARMONI dedicated to high-resolution imaging and spectroscopy in the near-infrared spectral range. The MAORY instrument module will implement Multi-Conjugate Adaptive Optics to deliver to MICADO a wide field-of-view corrected from the atmospheric turbulence. METIS will be the only instrument to observe in the mid-infrared range,[1] from 3 μm to 13.5 μm, and deliver diffraction-limited imaging and high-resolution spectroscopy simultaneously in this wavelength range.

Further author information: (Send correspondence to Monika Rutowska)
E-mail: rutowska@ph1.uni-koeln.de, Telephone: 0049 221 470 7791

Ground-based and Airborne Instrumentation for Astronomy IX, edited by Christopher J. Evans, Julia J. Bryant, Kentaro Motohara, Proc. of SPIE Vol. 12184, 121843M
 · 0277-786X · doi: 10.1117/12.2630802

The science cases covered by METIS will be very diverse, ranging from the study of nearby exoplanets and proto-planetary disks to the study of high-red shift galaxies and the Galactic Center. It will be an ideal complement to existing facility like ALMA[2] and recently launched the James Webb Space Telescope.[3] METIS is built by a large consortium of European research institutions led by NOVA in the Netherlands with each partner responsible for a sub-system of the instrument. The full assembly and integration of the instrument will take place in Leiden before shipment to Chile, at the summit of Cerro Armazones.

One sub-system of METIS is the so-called Warm Calibration Unit (WCU) developed at the University of Cologne. The main role of the WCU is to supply METIS with functionalities able to test, calibrate and trouble-shoot the METIS instrument as a whole. In this sense, several artificial sources will be provided by the WCU to calibrate the detector response, to test the delivered image quality and understand the performances of the high-spectral resolution LMS subsystem. This paper describes the conceptual principle of the WCU and details the adopted design in view of the next important milestone for the METIS project, namely the Final Design Review planned in November 2022.

2. OVERVIEW OF WARM CALIBRATION DESIGN

2.1 General overview and functionalities of Warm Calibration Unit

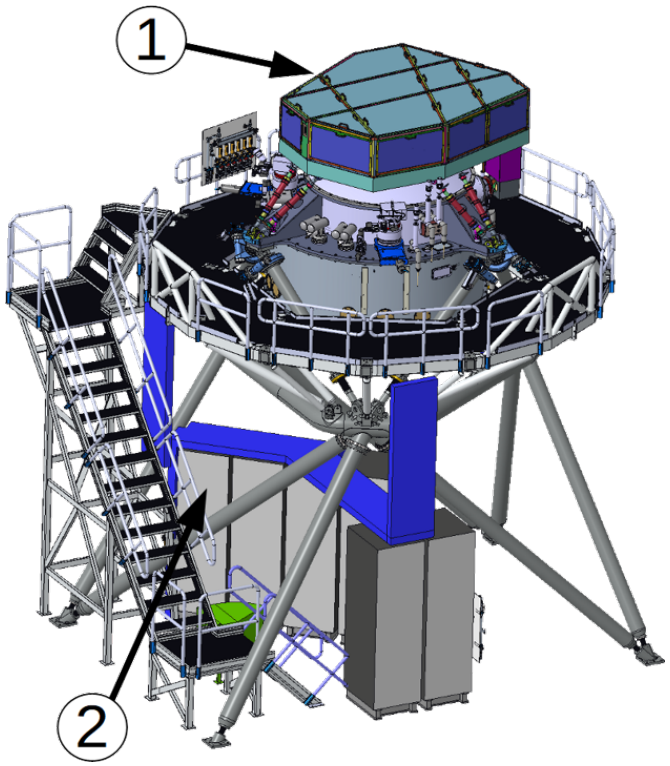

Figure 1. Schematic view of the METIS instrument. The WCU is positioned above the cryostat and the Laser Cabinet on Nasmyth platform (1: Main Opto-mechanics, 2: Laser Cabinet)

Physically the WCU consists of two parts. The adjustable main part (1) contains most of the opto-mechanical devices placed on the optical bench, which stand above the cryostat on the hexapod. In Fig. 1, the WCU bench is fully covered by the WCU enclosure. Fig. 2 shows the internal view of the WCU without the enclosure. The second part (2) is the laser cabinet. Inside the cabinet are the laser sources assemblies. The cabinet itself is placed on the Nasmyth platform.

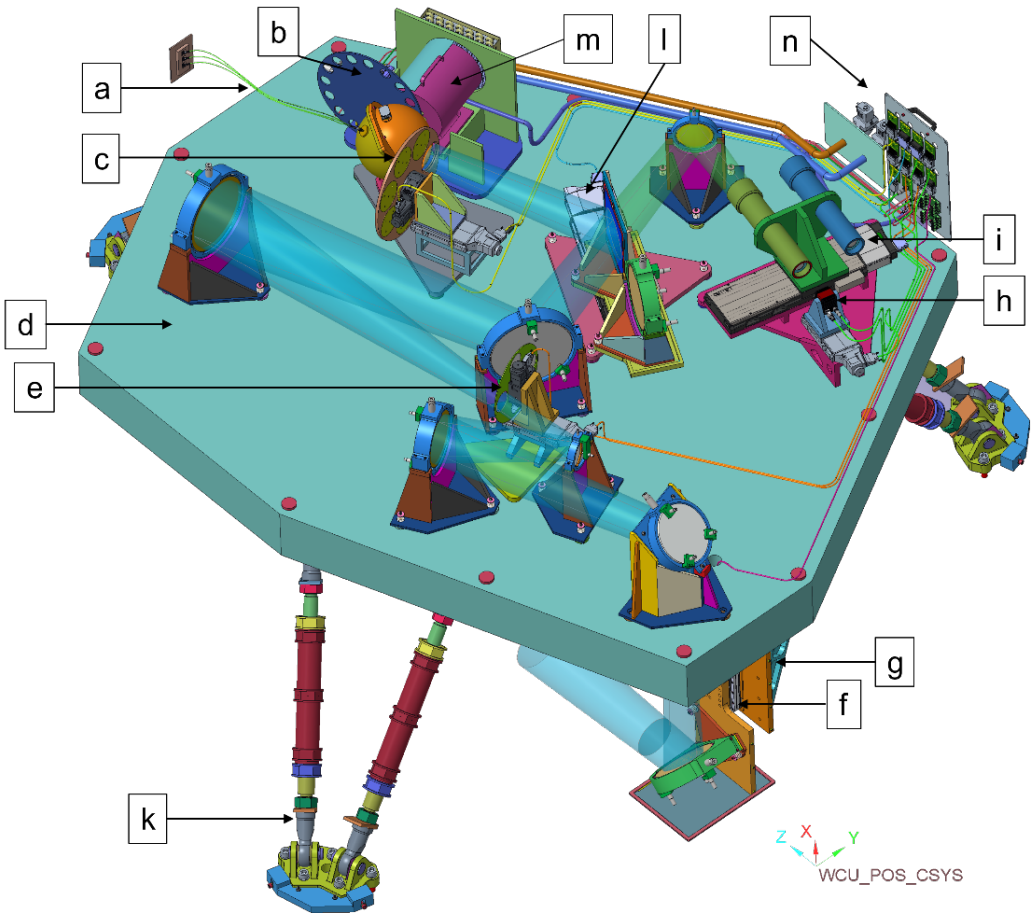

Figure 2. Overview of the main components of the WCU (enclosure is not shown), a blue color cylinder indicates the optical beam.

Connecting both the parts will be an encased electrical cable tray (shown in dark blue in Fig. 1) and another tray with the optical fibers. The electrical cable tray connects the electrical WCU devices to the ICS. The fibers (a) guide the light from the laser sources into an integrating sphere inside the WCU. The second type of light source is the blackbody (m). It is broadband light source and has been selected for a stable source flux. The aperture mask wheel (b) with different apertures allows controlling the light flux, which enters the integrating sphere. The light flux is represented in Fig. 2 with a semi-transparent, blue, cylinder shape. At the output port of the integrating sphere is another wheel with several pinhole masks (c) mounted on a linear stage to adjust the focus. In the accessible pupil plane of the Offner relay, a third wheel (e) allows switching between four different pupil stops. Most opto-mechanical elements in the main part of the WCU are going to be mounted on a lightweight CFRP bench (d), which in total cover about 70 % of its total area. The second structural part is a periscopic arm (g) which is shown in Fig. 2 without its enclosure and in open position. Its selection mechanism (f) slides down a part of the periscopic arm and a fold mirror is placed in the optical path. Then, the WCU beam can enter the cryostat. Afterward, the mirror is slide up and the periscopic arm is fully closed. The ELT beam can then enter the cryostat. During system MAIT, an additional selection mechanism (i) moves one of the two objectives in a front of the CCD, while a third selection mechanism (l) switches from a fold mirror to a beam-splitter to allow the full alignment functionalities of the WCU. The focusable CCD camera (h) delivers an optical feedback to the Instrument Control System. The electrical cables and the water pipes are connecting the WCU devices to the WCU-ICS panels (n). The whole WCU bench is mounted on the hexapod (k) attached to the stiff ring of the cryostat.
For final design of the WCU we have aimed to keep the total weight of the WCU within 1300 kg (with 10 %

margin) and the WCU devices of the Laser Cabinet under 100 kg.

2.2 Aperture mask prototyping

In this paper, we present the most recent lab tests of the aperture masks.

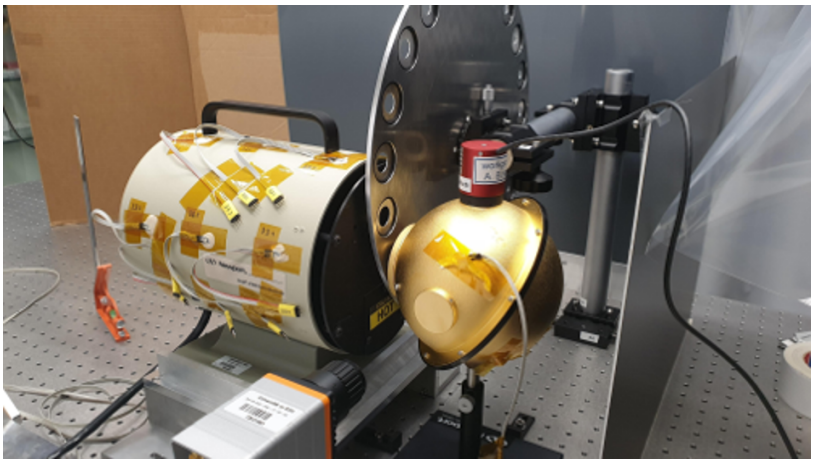

Figure 3. A photo of the setup: the blackbody source, the aperture masks wheel and the integrating sphere.

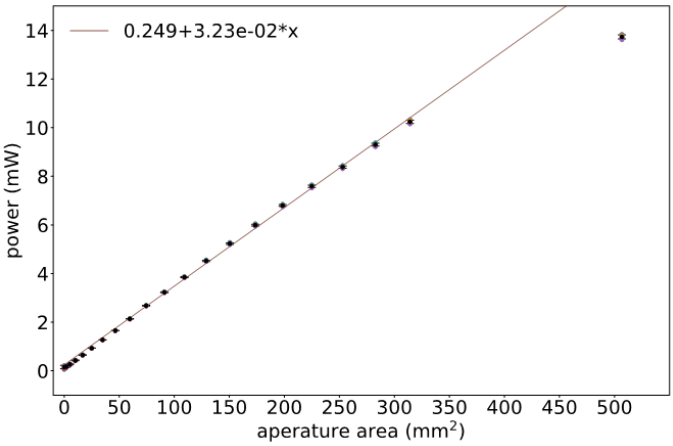

Figure 4. The aperture mask test results where the mean flux measured by the power-meter is plotted against the aperture area. The repeatability – lies between 0.5% to 0.7%

In order to perform the detector linearity tests for METIS it is foreseen to tune the blackbody flux output by 15 repeatable steps and with one 'closed' step. For this, we foresee to have a wheel placed between the blackbody output (25.4 mm diameter) and the integrating sphere input (25.4 mm diameter). Recently, we tested a 3 mm thick aluminum wheel, which contain 21 ports. One mask fully blocks the blackbody output flux. One of the mask has the largest open diameter 20 mm. It gives us 20 masks with diameter between 0.2 mm to 20 mm with a step of 1.00 mm. Each mask was made of 1 mm thick aluminum.
The wheel with an attached rotation stage was placed between the blackbody source, warmed up to 1000°C, and the integrating sphere. Fig. 3 shows a photo of this setup. At top of the integrating sphere is attached a thermal sensor, Thorlabs, S302C. The wheel position and the power readout were remotely controlled.
The plot of Fig. 4 shows one of such tests with calculated the average power collected for 3 min for each mask. At x-axis is calculated open area of the mask. At the y-axis is the power in mW unit. We observe a linear

relationship between the aperture area and the measured power. The slope for 19 masks is less than 0.03 and the calculated repeatability is in the range of 0.5% to 0.7%.

3. MAIN MECHANICAL COMPONENTS

WCU will be in operation only during daytime. Operational temperature range is from 0°C to 15°C. No stable temperature inside WCU is foreseen and no thermally resistant enclosure. WCU should be not warmer than 2.5°C or colder than -8°C in a comparison to temperature inside the ELT dome. In order to reduce any thermal effects all WCU elements are expected to be made of a very low CTE materials (as CFRP, Zerodur glass and invar) and matching between each other as close as possible. Following this and weight restrictions it is planned that WCU bench is made of CFRP material.
Moreover the WCU is attached to METIS by a six symmetric adjustable links to minimize focal and pupil misalignment due to temperature changes.
In this paper we present the current, FDR, hexapod design and its prototype tests. We discuss the changes and improvements of the CFRP bench and the mirror mounts designs in comparison to the WCU papers presented in SPIE 2020 conference.

3.1 Hexapod - Adjustable Link

Fig. 5 shows a top view of bare WCU optical bench attached to METIS by the hexapod. Around the WCU is the WSS RIG platform. A distance from a top surface of the RIG platform to a top surface of the WCU bench is 1860 mm, when the WCU is at its nominal position. The hexapod and the bench current design has taken into consideration convenient access to the hexapod and its interfaces, and METIS PTCs.

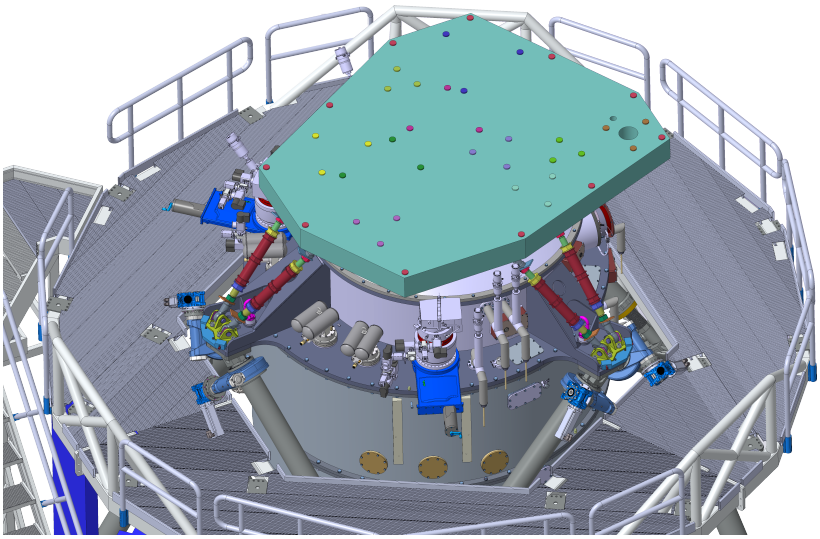

Figure 5. View of bare WCU optical bench placed on METIS by the hexapod with the RIG platform around WCU.

One of the main functions of the hexapod is the alignment of the WCU to the CFO focal and pupil planes. This drives travel range requirements as: ±26 cm in x-axis, ±25 in y-xis, and ±55 in z-axis, and rotational adjustment as: ±1.7° in x-axis, ±1.6° in y-axis, ±1.6° in z-axis for the hexapod. This hexapod cover all required travel range. Moreover, the hexapod accuracy shall be in the range ±330 μm and the repeatability ±49 μm in order to align the WCU focal and WCU exit pupil planes to CFO focal and exit pupil planes, respectively.

Fig. 6 illustrates in detail a cross section of one link. Bearing ends (grey color) are heavy-duty rod for high radial loads with two rotational degrees of freedom. The middle part (dark red color) is a telescopic cylinder. The sizes of the piston (yellow color) and the piston tube (green color) have been calculated based on the earthquake and the eigenfrequency analysis. The length of the hexapod links is adjusted by rotating the telescopic cylinder,

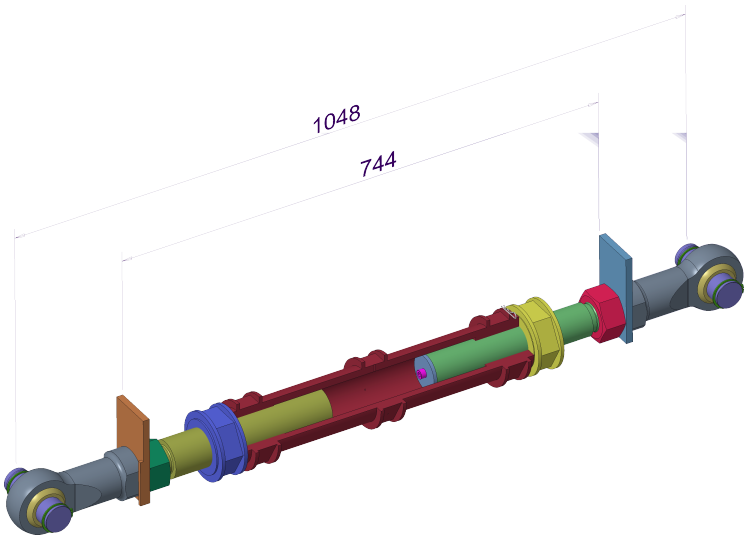

Figure 6. WCU hexapod link, with section view and dimensions for better understanding .

which has internal M42x2 threads.

- Stainless-steel was selected as the main material for this construction
- Total length of the link (in nominal WCU location) is 1048 mm
- One link weight 35 kg

Two square shaped plates locked at the bearing end, at lower (orange color) and at upper (blue color), are designed for mounting a laser distance measure device. This length measurement is required for precise alignment of the WCU with the METIS.

3.2 WCU interface to the Cryostat structure

The CRY-WCU mechanical interface is divided in two parts:

- permanent connection between the WCU hexapod and the stiff ring: bracket
- non-permanent connection between the WCU hexapod and the stiff ring: jig

The bracket is shown in Fig. 7 as a light green part connecting two links. The bracket is made of a stainless steel and attached to the cryostat by 5 x M20 screws. It was calculated that a required tightening torque is 436 N·m for sustaining the earthquake loads. Once attached the hexapod are not foreseen to be removed from the brackets. A pink ring structure in Fig. 7 placed behind the bracket is a locking system. In case of assembling / disassembling the WCU the hexapod will not changed its position and length.
The jig is shown in Fig. 7 as a blue attached to the front of the bracket. The jig is made of a stainless steel and attached to the bracket by 2 x M8 screws. It was calculated that a required tightening torque is 34 N·m.This part is used for the aligning the WCU onto the cryostat structure. When the WCU and the brackets are fixed onto the cryostat, the jig is removed.

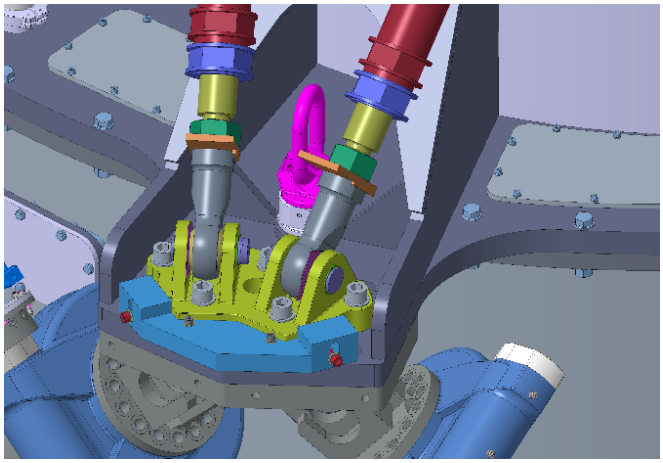

Figure 7. Zoomed-in section of one of the interfaces, where the jig is shown with a blue color and the bracket with a green color

Figure 8. Photo of the setup: the link attached at lower and higher bearings to the frame.

3.3 Preliminary tests of adjustable link

Parallel to calculations and FEA analysis for the hexapod, one adjustable link of size and dimensions following the last design of the hexapod got manufactured by the mechanical workshop of I Physics Institute in UzK. Several tests were performed for the link. The link is attached at the lower and the upper ends to form the basic beam, the upper end of the link is loaded with the help of a lever (see Fig. 8).

At the free end of the lever, we placed in total 90 kg. By the leverage effect the link get loaded with 5 kN load. This is maximal weight load we expect and under which the hexapod link need to get adjusted. A dial gauge is placed at the top of the setup to monitor the change in the length of the link.Then, the measurement of any changes of the link length were monitored for 10 days to look for the settling effects. None was observed. In addition, the link was exposed to the vibrations of a human jumping around on the floor next to the test setup. Also here, no change of the link length was recorded. Other important tests were the resolution tests with different lubricants on the threads. Resolution here means, what is the change in length one achieves after overcoming the sticking in the thread, slipping and sticking again at the new position again. Also, this experiment was done in the lab, where the operating person can stand comfortably, upright, next to the setup.

Table 1. Results of step size for different lubricants with load

	Re-oiled	Greased	Coated with PTFE
Max. step width (μm)	45	28	18
Average step width (μm)	28	17	9
Estimated torque (N·m)	94	59	

Table 1 shows the results for the different lubricants. We tested the link with 90 kg load. Applying PTFE on the thread delivered the best result. Nevertheless, the average step size for all lubricants in the loaded situation is lower than the required step of 60 μm. The minimum step size has been calculated that in order to fulfill the focal co-alignment in range of ± 0.33 mm in x-axis and y-axis a minimal change of one link should be ± 60 μm.

3.4 CFRP optical bench

It has been chosen to employ CFRP material for the optical bench. The CFRP was preferred over a more standard aluminum bench for a number of factors. The most important is that, for the same requirements on stiffness and optical performance, an ALU bench would be more than twice as heavy as a carbon fiber one, therefore requiring an even heavier hexapod to support it. In addition, CFRP is characterized for having a very low CTE, which is a desirable feature that allow us to minimize the level of compensation needed to counteract the thermal expansion that inevitably happens during operation at the telescope.
Fig. 9 presents the WCU optical bench. This design was further taken into the gravity loads modeling using finite element methods analysis. Internal structure of the bench is made of CFRP ribs and a foam. At top and bottom are two cover-plates. The size of the bench is asymmetrical with height of 200 mm x longest side 2905 mm x widest side 2410 mm. The estimated weight is up to 230 kg. CTE of the bench is estimated as: 2.5 x 10^{-6} mm/mm·K unidirectional.

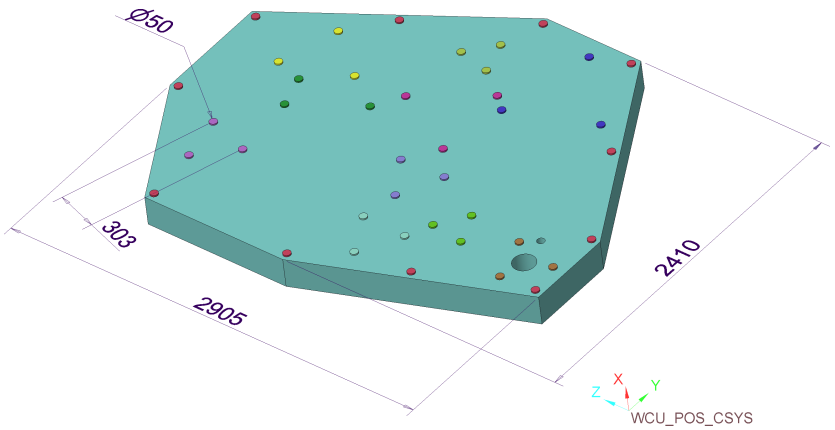

Figure 9. WCU optical bench with shown interface points for the devices placed onto the bench as the mirror mounts and linear stages.

Interface contact pads, shown in Fig. 9 as circular shape, with 50 mm diameter are color-coded for the WCU devices. For each device such as the mirror mounts and stages, the interface consists of three pads. These three pads in each group are placed on a triangle, whose vertices are located on a circle, the radius of the circle is decided considering factors such as alignment tolerance requirement. There are dark red color pads along edges of the bench. These pads are for mounting the enclosure frame. During the bench fabrication, the contact points are glued and milled into the CFRP with a precision better than $\pm$ 30 μm. This allows for the opto-mechanical elements (such as assembled mirror mounts) to be mounted directly onto the bench without the need of alignment. Fig. 9 also shows a circular hole on the right side of the bench, which allows the light to travel from periscope fold down mirror towards the WCU feed mirror.

3.5 Periscopic arm

On left side of Fig. 10, we present the WCU periscopic arm when viewing from the front and in open position. The center of the feed mirror is centered to the ELT optical path. When the WCU is in operation, the WCU beam is reflected to the Cryostat window. When not, then the mirror assembly is slide up and the periscopic arm is fully closed.
The periscopic arm support structure attached to the CFRP bench (triangular, rose color structure in Fig. 10), interface to a linear stage (yellow color) and interface between the linear stage to the mirror mount (light yellow color) are made of aluminum. The choice of the material was driven by a material of the stage. Because all of these elements has the same CTE, then all of them would behave the same way to any temperature changes. On right side of Fig. 10 is illustrated the back view of the periscopic arm in closed-in position. In this Fig. 10, we show a concept of attachment of aluminum supporting structure to the CFRP bench. There are three pins which decides the location and the orientation of the periscopic arm. Whole periscopic assembly is attached to the bench from below and is locked in its position with the help offspring loaded screws. This concept is similar to the mirror mounts where the part retains its location, although the different parts can change their sized because of the temperature.

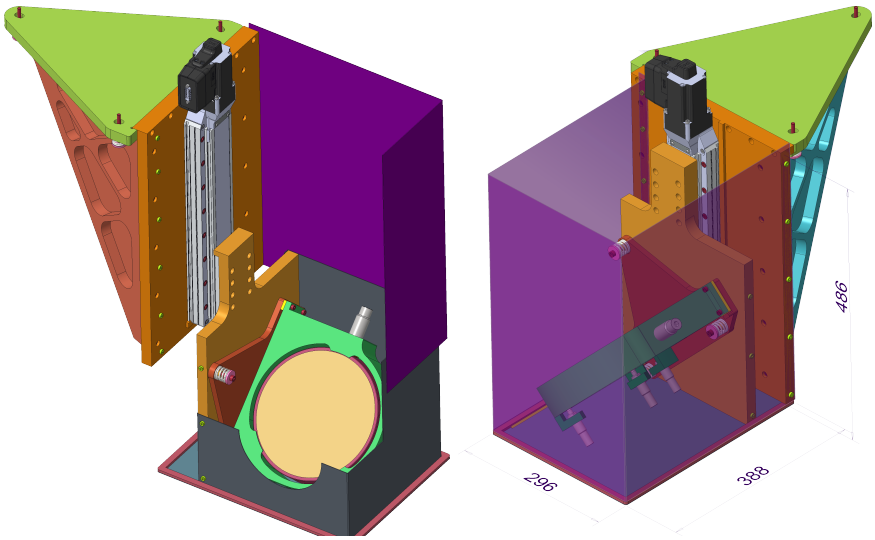

Figure 10. Representation of the WCU periscopic arm assembly; on left side is a front view and open-in position and on right side is a back view and closed-in position.

The feed mirror assembly is the only part in the periscope arm, which is not made of aluminum. The mirror is made of Zerodur glass, and the mount is Invar 36. The mirror is tilted at 45° to x-axis (MRF).The mirror assembly is attached to the interface plate by three locating pins. The mirror is hold in the mirror cell by three spring loaded plungers.
This interface plate is hold by a linear stage and another interface plate. For the linear stage, we chose Zaber stage, model: LRT0250AL-E08CT3A with 250 mm travel range.
The total weight of the periscopic arm is less than 50 kg.

3.6 Mirror mounts assembly

Fig. 11 represents the design of the mount for CM1 mirror, which is one of the largest and spherical mirror. The right side shows a front side of the mirror (yellow) mount, which illustrates a protected gold coating. The clear aperture of the mirror is marked with a black circle of 248 mm diameter. The center of the mirror is at 287.5 mm high from the bench top surface. In a front, two grey color triangular shapes are the mount supporting ribs. Location and orientation of the mirror mount on the bench is defined by three locating pins, which are inserted

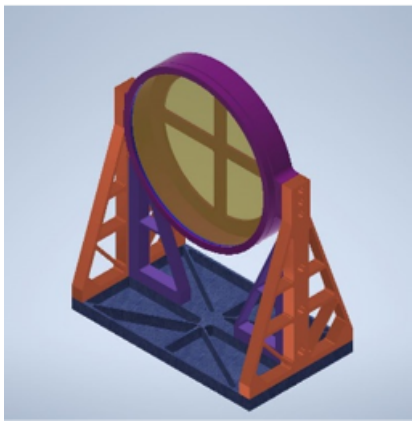

Figure 11. The mirror mount concept design as for CM1 mirror (the largest, spherical one)

inside the interface pads on the bench. Spring loaded screws are used to lock the mirror mount to the bench. The spring force is decided so that the mirror mount do not move out of its position even during the earthquake loads. The locating pins are located on the vertices of an equilateral triangle, these three vertices define a circle. The distance between any two pair of pins is 303 mm. This distance was chosen after carefully going through the tolerances, which can be tolerated by the optics, and the manufacturing tolerances.
Holes for the locating pins in the base plate of the mount are not circular but are in the shape of a slot. These slots are oriented towards the center of the triangle made of three slots. These slots basically allow to compensate for any mechanical misalignment or stress arising out of the differential CTE between the bench and mount material.
Left side of Fig. 11 shows a back side of the mirror (white) with three spring loaded plungers, which holds the mirrors inside the mirror cell. Front side location of the mirror is defined by the three flat pads machined into the mirror cell (circular blue part). These axial plungers only restrict the mirror movement in the axial direction. A similar plunger, with higher spring force locks the mirror in direction perpendicular to the bench surface. Here, we would like to point out that, the spring force for the plungers is decided such that the mirror is not displaced from its location even during earthquake loads.
Another important aspect of the mirror cell design is related to the contact stresses, which can be safely applied to the Zerodur substrate with damaging it. Here, the pads, which comes in contact with the Zerodur surface, are dimensioned such that the contact stress is always below 25 MPa.[4]

It is planned that all mounts are manufacture of nickel-iron alloy (Invar 36). One of advantages of employing this alloy is uniquely low CTE 1.3 x 10^{-6} mm/mm·K. One of disadvantages is its high density (8.1 g/cm^3) , for example this CM1 mirror mount's weight is close to 26 kg (without any pocketing, few kg can be saved with pocketing).

3.6.1 Locating pin

Fig. 12 shows the section view of one of the contact point between the mirror mount and the bench. Below are the different parts of this assembly:

- Pad (purple color) is 10 mm thick and 50 mm diameter, it is made of stainless-steel
- Pin (yellow color)
- Spring (white color)
- Washer (pink color)
- Screw (grey color)
- Bush (green color)

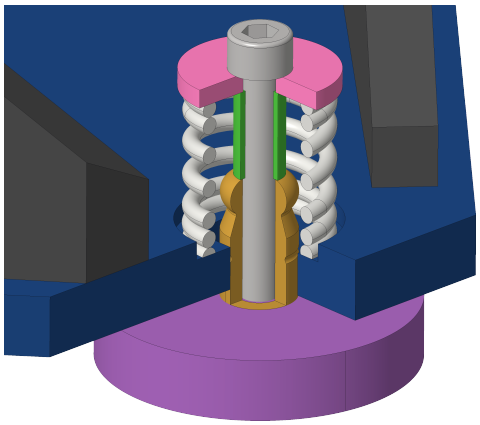

Figure 12. Cross-section of the locating pins placed into the mirror base.

The interface pads (shown in purple) are glued to the bench by the bench manufacturer and are milled to an accuracy of $\pm$ 30 μm. The interface pad has a hole in it, where a locating pin with hole is mounted. Once three locating pins are in place, the mirror mount is placed on the bench, with orientation and location decided by these three pins. Next step is to put the spring, bush, washer and the screw to fix the mirror mount on the bench. Important point here to note is that this kind of interface locks the mirror mount on the bench, however, it allows the mirror mount and CFRP bench to move relative to each other (with mirror surface always remaining at the center of the triangle) to compensate for the differential CTE.

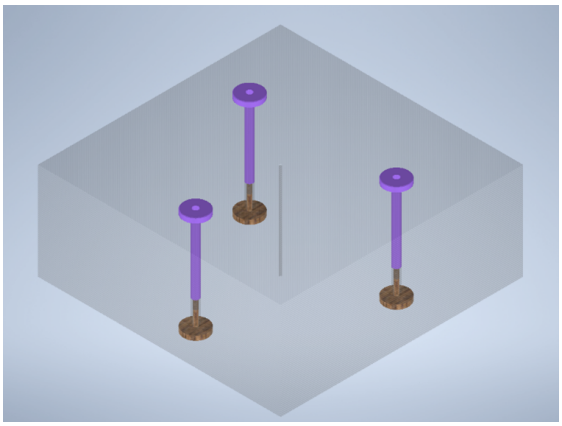

Figure 13. Attachment of the locating to the CFRP bench (semi-transparent cube).

Fig. 13 illustrates the concept of attachment of the interface into the CFRP bench (shown as semi-transparent cube). This concept basically consists of two parts coming from top and bottom and bottom and screwed together. These pads are additionally glued to the bench surface. This concept of interface pads was discussed with the CFRP manufacturer, who sees no issue with this.

4. THE WCU LASER CABINET

As it is shown in Fig. 1, the lasers and its items are a separate unit named: the WCU Laser Cabinet. It is located on the Nasmyth platform and connected to the WCU by the optical fibers. The cabinet is NVent Schroff LHX3, 2.2 m high, 38 units with vibration insulators and ESO seismic frame without thermal insulation. It is the same cabinet as the Instrument Control Sub-System (ICS) cabinets and one of six cabinets placed on Nasmyth platform next to the METIS.

Inside the cabinet are the three lasers' assemblies. These lasers are foreseen to be the calibration sources for the LMS mostly for AIT phase. The daily wavelength calibration of the LMS will be covered by collecting telluric sky lines. Due to the fact that there is no need to examine the LMS over a full spectral range during AIT, the most significant region of interest to the LMS were chosen, as follow:

1. Blue end around 3 μm
2. CO lines around 4.65 μm
3. Red end around 5 μm

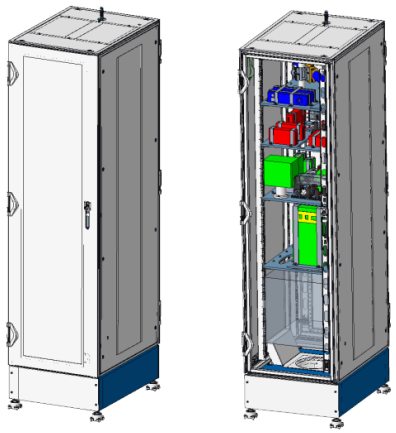

Figure 14. Images of CAD design of the laser cabinet, at left side is the cabinet closed and at right side is opened.

Fig. 14 shows the design of the laser cabinet, where at the left side is presented the closed cabinet. At the top of the cabinet, it can be noticed a short piece of the fibers. There three IR fibers, which connect the laser sources in the cabinet to the WCU integrating sphere. At the right side is shown the opened cabinet with three lasers assemblies. The color of the assemblies follows its role of the wavelength range calibration:

- at top is a blue color Laser I assembly, which covers the blue LMS end
- at second top floor is a red color Laser III assembly, which cover the red LMS end
- below we find a green color Laser II assembly. It covers the middle range of LMS. The laser head requires to be connected to a water chiller. The chiller is placed below the Laser II assembly floor together with a piezo-controller

4.1 Laser I assembly (blue end)

Fig. 15 shows an isometric overview of the laser I assembly. The main parts of this assembly placed on the board are:

- Monochromatic laser, model: REO-32172, CW, HeNe operating at 3.39 μm, (shown as long blue tube)
- Laser controller, model: REO-39785, (blue rectangular box)
- Optical setup
- The fiber (to a top of the cabinet 870 mm long) and fiber baffle

- Board (435 mm x 10 mm x 510 mm)

The HeNe laser head is placed onto the board along a diagonal line. At the laser hear aperture is an optical shutter. Then, the laser beam is reflected by a mirror to a long-pass filter at 3.1 μm and focused to the SMA fiber by a plano-convex lens with a 50 mm focal length. Optical setup is covered by a baffle. This baffle is semi-transparent only for a presentation purpose. The baffle will be blackened and fully covering the laser beam, following the laser safety requirement. The reason to have the baffle, excluding the laser safety, is a protection of any optical element from the dust and contamination, which may occur over time. The third reason is to protect the laser beam from the air flow. At top of the cabinet a fan is installed. It is our intention to keep a constant air flow in the cabinet in order to stabilize temperature within the cabinet to ambient temperature inside the ELT dome.

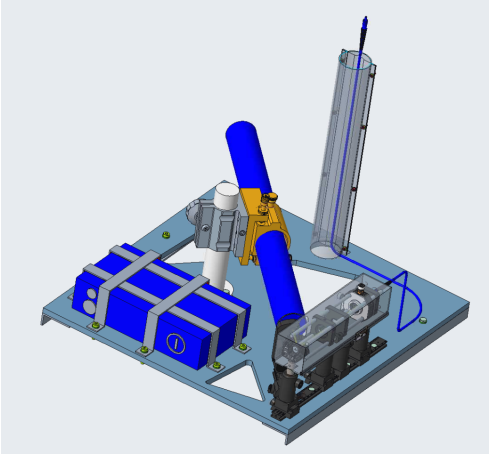

Figure 15. Isometric overview of the Laser I assembly

4.2 Laser II assembly (CO fundamental transitions lines)

Fig. 16 shows items of the Laser II assembly without the chiller, which is placed below the Laser II assembly.The main parts of this assembly placed on the board are:

- Tunable QCL laser, Daylight Solution, model: CW MHF, center wavelength at 4.65 μm with a tuning range around 200 nm
- SideKick controller together with its power supply
- Wavemeter, Bristol 771
- Optical setup
- The fiber (to a top of the cabinet 1320 mm long) and fiber baffle
- Breadboard

Similar to the Laser I assembly in the front of the laser head is placed an optical shutter. The laser beam is split by a beam splitter, where 50% of the beam is focused into the fiber by a plano-convex lens with a 50 mm focal length. Another 50% is reflected by a mirror into the wavemeter. Each generated wavelength is read out simultaneously by the wavemeter.

Another two items of the Laser II assembly are attached on an additional board below the laser II assembly:

- The chiller, ThermoTek, model: T257P
- Piezo controller, Thorlabs, model: MDT694B

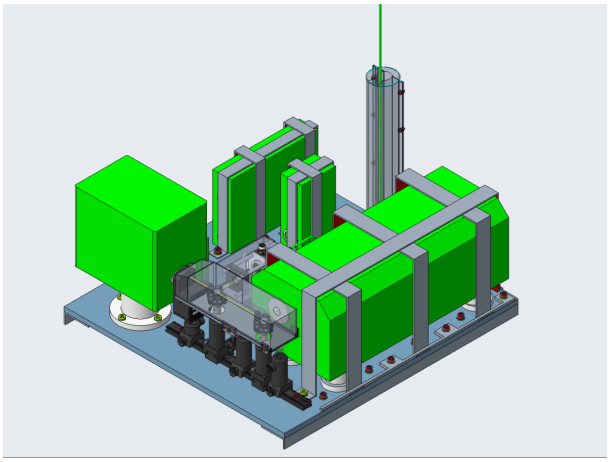

Figure 16. Isometric overview of the Laser II assembly

4.2.1 Laser III assembly (red end laser)

Fig. 17 shows the Laser III assembly. The main parts of this assembly are:

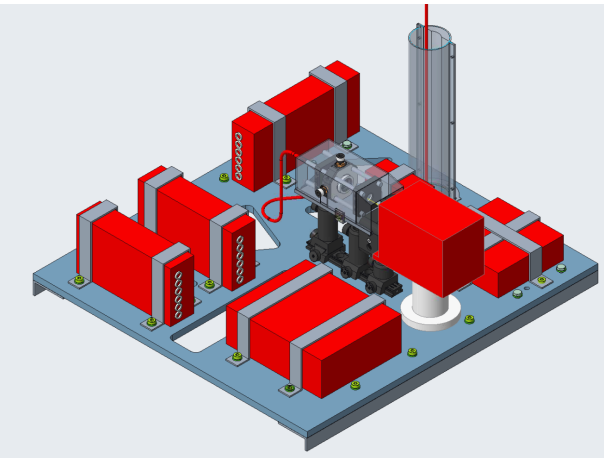

Figure 17. Isometric overview of the Laser III assembly

- Hamamatsu, Distributed Feedback Quantum Cascade Lasers (DFB QCL) laser at 5.26 μm, model: L-12005-1900H-E
- The laser is placed inside HHL mount, Hamamatsu, model: A11134-07
- The power supply for HHL mount, TDK Lambda, model: HWS15A-12/A
- Temperature controller (TEC), Hamamatsu, model: C11330-01
- The power supply for TEC controller, TDK Lambda, model: HWS100A-24/A

- Laser driver and current controller, Wavelength Electronics, model: QCL1500 (+) OEM
- Two power supplies for the laser controller, model: Wavelength Electronics, model: PWRPAK 24V
- Optical setup
- The fiber (to a top of the cabinet 1050 mm long) and the fiber baffle
- Breadboard

Similar to described two laser assemblies in the front of the laser head is placed an optical shutter. The laser beam is directly focused to the fiber by a plano-convex lens with a 50 mm focal length.

4.3 Optical fiber connections

The optical fibers transmit the lasers' signal from the WCU laser cabinet to the WCU main structure. Three described above fibers, coming out of three specified above lasers, are set together inside one protection tube. The fibers' tube is attached to WSS structure and tracked to the top of the WCU enclosure. Due to manufacturing limitation there are two pieces of these fibers 4 m + 5 m connected between each other by SMA sleeves. At the WCU enclosure are three SMA connectors. The connectors connect the fibers to the fiber bundle inside the WCU. Such solution allow to connect any SMA fibers to the WCU and the same feed the WCU integrating sphere with any laser source without opening the WCU enclosure.
The fiber bundle enables delivery of three laser sources in a single SMA connector. The fibers are placed in the bundle side by side, and at the very end are fused. At the WCU integrating sphere can be only one port for the SMA connector. It is estimated that a length of the fiber bundle from the integrating sphere to the enclosure is around 70 cm.

We propose to use a hollow-core optical fiber, manufactured by Guiding Photonics Company, US. The fiber core is a hollow and its internal side is covered by a dielectric layer: silver-lodide (Agl) and outer side is a reflective silver layer. Around the hollow core are protective layers as glass/plastic capillary and a protective buffer. In addition, the patch fiber will have an extra stainless-steel tubing. Such fiber transmits infra-red beam with lower loss of the signal in a comparison to a solid core MIDIR fibers. For the above described lasers' and its operation range (3.39 μm, 4.65 μm and 5.26 μm) we propose to use a hollow-core fiber of 500 μm core diameters. It transmits more than 95% of the signal per 1 m of the fiber.

4.4 Lab tests of the HeNe laser and the fiber coupling

The coupling between the HeNe laser and the MIDIR fiber was tested multiple times, using different lenses. Here, we present the laser transmission results for two different fiber length: 5 m and 10 m.

In Fig. 18 we see, the HeNe laser head (tube with a yellow label), next to it is the long pass filter and a plano-convex lens, 20 mm focal length (Thorlabs, LA5315) and the SMA1 SMA fiber holder placed into Thorlabs, CXYZ05/M X, Y axes adjustable holder. Another end of the 5 m fiber is placed in the front of the power meter sensor: Thorlabs, S302C. (see: right side of Fig. 18).
After aligning the laser and placing the long pass filter the laser power was measured as 4.34 mW. The power meter sensor was placed at 140 mm distance to the laser head. It allows us to later on calculate the ratio of the transmitted power by the 5 m or 10 m fibers including the coupling, the fiber bending and the SMA sleeve losses.

Left side of Fig. 19 shows transmission curve of the HeNe laser with 5 m fiber. The fiber output end was placed in a front of the power meter sensor. The input laser decreases of 50%. Average power over 5 min measurement was 2.22 mW $\pm$ 0.019 mW. Then, the fiber 1 output was disconnected from the power meter and connected to SMA-SMA sleeve. Another 5 m fiber was connected to the sleeve and the fiber 2 output was placed in the front of the power meter sensor. Right side of Fig. 19 shows transmission curve for this setting. The input

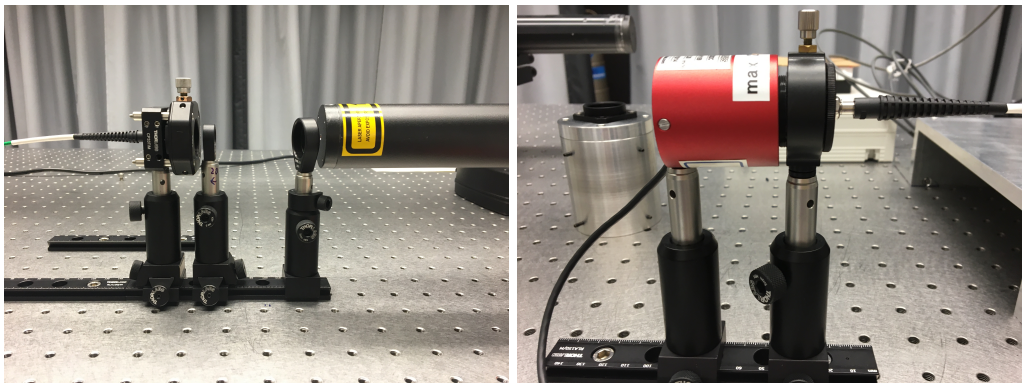

Figure 18. Left side photo of the optical setup: HeNe laser, tilted long pass filter, 20 mm FL lens, and the fiber in the fiber holder, on right side is a photo of the fiber output in the front of the power meter sensor

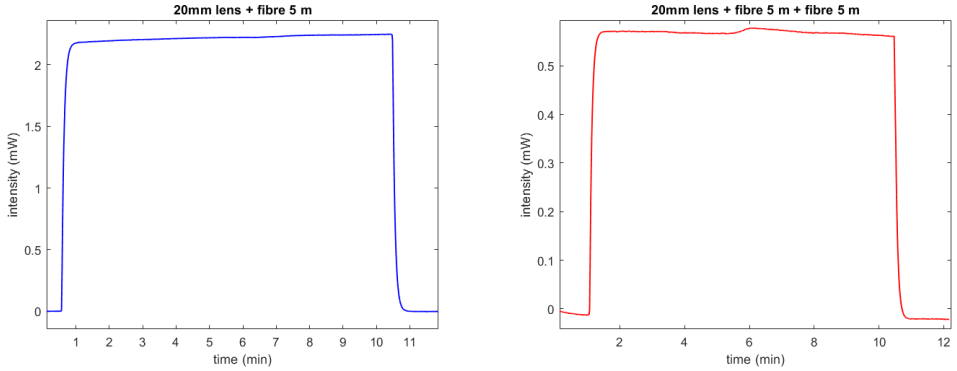

Figure 19. Left side graph is a transmission curve of 5 m fiber and 20 mm FL lens with the HeNe laser ; right side is a transmission curve of 5 m fiber + SMA-SMA sleeve + 5 fiber and 20 mm FL lens with the HeNe laser

laser dropped power by 87%. Average power over 5 min measurement was 0.57 mW $\pm$ 0.004 mW. Taking into calculations transmission losses of 1 m of this fiber as 0.5 dBm, more than 95% of the coupling efficiency and the fiber bending losses, it is estimated that the SMA-SMA sleeve adds another 0.2 dBm loss. This number was confirmed by the fiber manufacturer.

5. CONCLUSIONS

The conceptual design of the Warm Calibration Unit of METIS and its current status have been presented and its main functions discussed. We have described the mechanical design of the WCU hexapod, the optical bench and the mirror mount. We have presented three laser assemblies placed inside the laser cabinet with the optical tests for HeNe lasers and the fibers. This WCU design will be submitted for Final Design Review in November, 2022. For a future work we are planning to complete design of the WCU lifting tools and supporting equipment and mature the assembly drawings to the manufacturing level.

ACKNOWLEDGMENTS

The work described in this paper has been partially supported by the German Federal Department for Education and Research (Bundesministerium für Bildung und Forschung - BMBF) under grant agreement (Verbundforschung) number 05A17PK2.

REFERENCES

[1] Brandl, B. R., Agócs, T., Aitink-Kroes, G., Bertram, T., Bettonvil, F., van Boekel, R., Boulade, O., Feldt, M., Glasse, A., Glauser, A., Güdel, M., Hurtado, N., Jager, R., Kenworthy, M. A., Mach, M., Meisner, J., Meyer, M., Pantin, E., Quanz, S., Schmid, H. M., Stuik, R., Veninga, A., and Waelkens, C., "Status of the mid-infrared E-ELT imager and spectrograph METIS," in [*SPIE proceedings*], Evans, C. J., Simard, L., and Takami, H., eds., **9908**, 990820 (August 2016).

[2] Wootten, A. and Thompson, A., "The Atacama Large Millimeter/Submillimeter Array," *Proceedings of the IEEE* **97**, 1463–1471 (August 2018).

[3] Gardner, J. P., Mather, J. C., Clampin, M., Doyon, R., Greenhouse, M. a., Hammel, H. B., Hutchings, J. B., Jakobsen, P., Lilly, S. J., Long, K. S., Lunine, J. I., Mccaughrean, M. J., Mountain, M., Nella, J., Rieke, G. H., Rieke, M. J., Rix, H.-W., Smith, E. P., Sonneborn, G., Stiavelli, M., Stockman, H. S., Windhorst, R. a., and Wright, G. S., "The James Webb Space Telescope," *Space Science Reviews* **123**, 485–606 (Novemeber 2006).

[4] Hartmann, P., "Minimum lifetime of ZERODUR® structures based on the breakage stress threshold model: a review," *Optical Engineering* **58**(2), 1 – 18 (2019).